Precipitation Forecast of MM5 in the Taiwan Area during the 1998 Mei-yu Season

FANG-CHING CHIEN

Department of Earth Sciences, National Taiwan Normal University, Taipei, Taiwan

YING-HWA KUO

National Center for Atmospheric Research,* Boulder, Colorado

MING-JEN YANG

Department of Atmospheric Sciences, Chinese Culture University, Taipei, Taiwan

ABSTRACT

This study presents precipitation verification, in the Taiwan area, for a real-time Pennsylvania State University–National Center for Atmospheric Research Fifth-Generation Mesoscale Model (MM5) system during the 1998 Mei-yu season. The highest equitable threat score (ETS) of precipitation forecasts, verified against observed precipitation, was about 0.2 at the 2.5-mm threshold for this nearly 2-month period. The complex and steep terrain in this region presented great challenges to the 15-km model in predicting realistic rainfall because the precipitation was driven by local forcings such as thermal effects and orographic lifting. In addition, the lack of observational data over the surrounding ocean greatly limited the quality of the model's initial data. It was found that the model system more accurately simulated nighttime rainfall than daytime precipitation. This was caused by the model underforecasting the rainfall events that resulted from solar heating and orographic lifting over the mountain slopes during the daytime hours. Precipitation, however, was overforecast over the high mountain regions (>1200 m). Further, the analysis of ETS with regard to the terrain height indicated that the model performed better over the lowlands than over the mountainous areas (slopes and highlands). It was discovered that the ETSs were much higher for precipitation forecasts after the onset of the east Asia summer monsoon than prior to the onset. Overall, the model more accurately predicted precipitation for the rainfall events associated with the Mei-yu front and the accompanying mesoscale convective systems than it predicted precipitation associated with the local forcings.

1. Introduction

An accurate precipitation forecast is one of the most challenging tasks in meteorology. Since the invention of numerical weather prediction in the mid 1950s, the overall forecast accuracy for temperature, pressure, and wind has shown steady improvement (e.g., Landis 1994; Kalnay et al. 1990; Shuman 1989). However, progress has been slow in the skill of precipitation forecasting (Olson et al. 1995). This is attributed to the fact that the physical processes responsible for producing precipitation are more complex than those that contribute to evolution of temperature, pressure, and wind. The complex, and ill-understood interaction of surface features such as topography, land–water boundaries, vegetation, and soil moisture are just some of the factors increasing the complexity of precipitation forecasting.

Despite its difficulty, accurate precipitation forecasting is very important to society. Because precipitation could adversely affect people's daily activities, their property, and even their lives, quantitative precipitation forecasting (QPF) was selected by the Science Advisory Committee of the U.S. Weather Research Program (USWRP) as one of the highest priorities for weather research (Fritsch et al. 1998). It was pointed out in the USWRP report that QPF will be a fruitful area of research for the foreseeable future, because of the development of new observation technology, the implementation of more sophisticated model physics, and the increase in computing power.

In recent years, many researchers have evaluated the accuracy of numerical models in QPF. For example, Johnson and Olsen (1998) assessed the QPFs issued by the Arkansas–Red Basin River Forecast Center during

Corresponding author address: Fang-Ching Chien, Department of Earth Sciences, National Taiwan Normal University, 88, Section 4, Ting-Chou Road, Taipei 116, Taiwan.
E-mail: jfj@cc.ntnu.edu.tw

May and June of 1995. Kato et al. (1998) verified precipitation forecasts produced by the 10-km nonhydrostatic mesoscale model of the Meteorological Research Institute in Japan. Mesinger (1996) showed that increasing horizontal grid resolution in the National Centers for Environmental Prediction (NCEP) Eta model resulted in an increase in QPF accuracy. Colle et al. (1999) evaluated cold-season precipitation forecasts produced by the 12-km Pennsylvania State University–National Center for Atmospheric Research Fifth-Generation Mesoscale Model (MM5) for the Pacific Northwest and found that precipitation was overforecast on the windward slopes and underforecast on the leeside slopes of major barriers.

Taiwan is one of the regions around the world that is frequently affected by heavy precipitation. Taiwan's complex and high-altitude terrain, which consists of steep mountain ranges such as the Central Mountain Range (hereinafter, CMR), with peaks exceeding 3000 m, is often a major factor in extreme-rainfall events (Fig. 1). When a front or a storm makes landfall on the island, the modification of airflow by Taiwan's topography can produce small-scale weather phenomena and result in enhanced precipitation on the mountain slopes. Typhoon Herb, which made landfall on northern Taiwan during 31 July and 1 August 1996, was a good example of a topographically enhanced precipitation event (Wu and Kuo 1999). During the period, a record-breaking rainfall amount (>1900 mm in 2 days) was observed at several stations on the CMR. As a result of the heavy rainfall, flooding and landslides caused severe damage over the island, and many lives were lost.

In addition to typhoon season, the other period of heavy rainfall for Taiwan, usually occurring from mid-May to mid-June, is called the Mei-yu (plum rain) season. Quasi-stationary fronts (the so-called Mei-yu fronts) frequently occur during the Mei-yu season. On satellite images, these Mei-yu fronts are usually associated with a long and relatively broad cloud band that extends from southern Japan southwestward to Taiwan and southeastern China. The Mei-yu fronts over southern China during this season are usually characterized by strong moisture gradients and horizontal wind shears, and most of them also exhibit baroclinic characteristics (Chen 1993). The low-level cross-front temperature gradients usually become weaker as the Mei-yu fronts arrive in Taiwan, because of modification of low-level thermal structure by the ocean. These Mei-yu fronts differ from those that occur over central China and Japan from late June to late July, because the latter are seldom associated with strong temperature gradients (Akiyama 1973; Kato 1985; Ding 1992).

Mesoscale convective systems (hereinafter MCSs) often develop and move along the Mei-yu fronts (Li et al. 1997; Chen et al. 1998). Many of them dissipate over the Taiwan Strait before reaching the island, but some MCSs last long enough to make landfall over Taiwan.
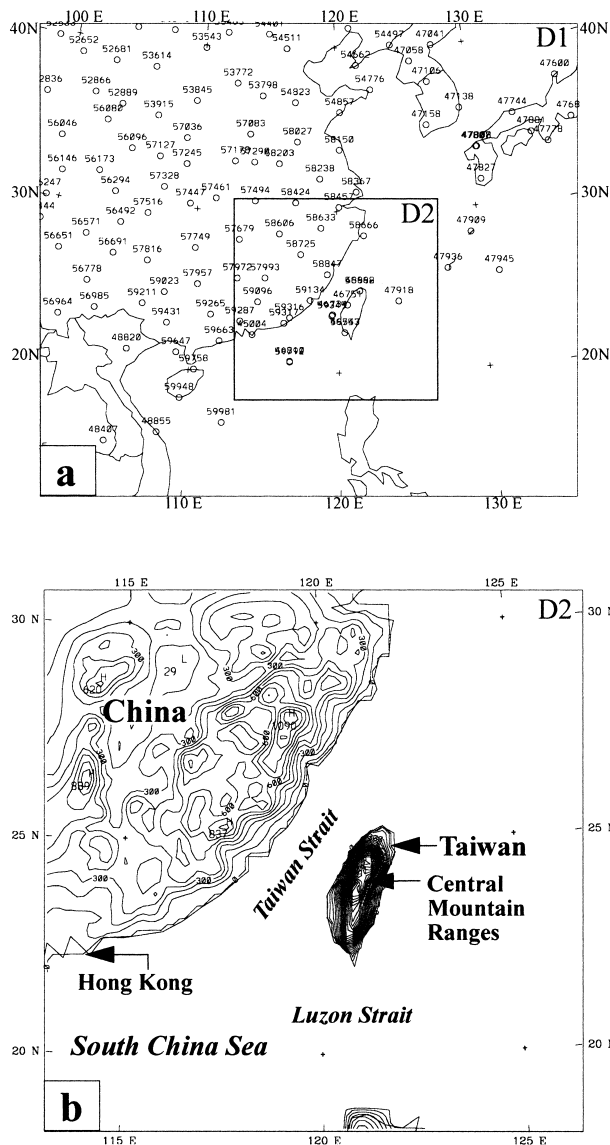

FIG. 1. (a) Domain configuration of the real-time MM5 system. The horizontal spacing is 45 km for domain 1 and 15 km for domain 2. Sounding stations are also shown. (b) Terrain height of domain 2, with a contour interval of 100 m.

When the landfalling MCSs encounter the high terrain of Taiwan, they can produce heavy rainfall.

Since TAMEX (Taiwan-Area Mesoscale Experiment), which was conducted over the Taiwan area in 1987 (Kuo and Chen 1990), several studies have been performed to improve our understanding of weather systems that produce heavy rainfall in the Taiwan area during the Mei-yu season. These studies have shown that heavy-rainfall events are frequently associated with surface fronts (Chen and Hui 1990; Ray et al. 1991), a midlevel vortex over northeastern Taiwan (Chen and Liang 1992), and MCSs (Wang et al. 1990; Lin et al. 1992; Li et al. 1997). Based on the findings from TAMEX and the rapid improvement of numerical weather

prediction models, researchers in Taiwan have begun to turn their attention to the improvement of quantitative precipitation forecasts. For example, Yang et al. (2000) studied the impact of model precipitation physics on rainfall prediction, using one of the heavy-rainfall events of the 1998 Mei-yu season. They found that precipitation prediction was very sensitive to the choice of cumulus parameterization schemes.

The Central Weather Bureau (CWB) in Taiwan currently operates a numerical weather prediction system that includes a global spectrum model (Liou et al. 1997) and a regional model (Jeng et al. 1991). As part of a collaborative project, known as the Advanced Operational Aviation Weather System, the Civil Aeronautics Administration (CAA) of Taiwan, the CWB, and the National Center for Atmospheric Research have, since 1997, been developing a real-time mesoscale forecasting system based on MM5. This real-time mesoscale forecasting system provides additional guidance for the forecasters at the CAA and the CWB and will be used to generate aviation forecast products. In this paper, we will examine the performance of this prototype mesoscale forecasting system in QPF during the 1998 Mei-yu season. In addition, the precipitation forecast accuracy of the model will be stratified in terms of daytime versus nighttime predictions, terrain height, and seasonal transitions.

2. Configuration of the real-time MM5 system

The configuration of the prototype CAA–CWB real-time MM5 system includes two domains with 45- and 15-km horizontal grid spacing, respectively (see Fig. 1). Twenty-seven sigma levels[1] are used in the vertical, with maximum resolution located in the planetary boundary layer. This system is run 2 times per day, at 0000 and 1200 UTC, each run lasting for 36 h. The initial (first-guess field) and lateral boundary conditions are supplied by the objective analyses and forecasts of the CWB global spectral model.

The objective analysis from the CWB global model is first interpolated to the MM5 grid. An objective-analysis procedure based on successive correction (i.e., the Cressman scheme) is then used to incorporate upper-air and surface observations into the initial data. The MM5 objective analysis is performed on the 45-km grid, which is then interpolated to the 15-km grid for model initialization. No further objective analysis is performed on the 15-km grid.

In the model simulations, the multilayer Blackadar (1979) parameterization is used to represent planetary boundary layer processes, including surface fluxes of heat, moisture, and momentum. The hydrological cycle includes the Kain–Fritsch (1993) subgrid-scale convective parameterization scheme and a grid-resolvable explicit moisture scheme in which cloud water, rainwater, and ice are predicted (known as the ''simple-ice'' scheme; Grell et al. 1994; Dudhia 1993). In addition, the simulations use the upper radiation boundary condition of Klemp and Durran (1983) to allow wave energy to pass through unreflected and relaxation of lateral boundary conditions to nudge the model-predicted variables toward the CWB forecast boundary condition.

3. Rainfall of the 1998 Mei-yu season

The observational data used for precipitation verification were obtained from 342 rain gauge stations,[2] spread geographically over the island of Taiwan (see Fig. 2 for locations). In general, the station density is relatively homogeneous over most of Taiwan, including the western slope of the CMR. However, the rain gauge stations over the ridge line and eastern portions of the CMR are sparse and inhomogeneous, which may induce error. Figure 3 presents the observed 12-h accumulated precipitation amounts averaged for all stations from 0000 UTC 6 May to 1200 UTC 25 June 1998. It is found that, before 17 May, rainfall occurred mostly during daytime, with almost no rain observed during nighttime. On these days, there were many afternoon thunderstorm events, which produced large amounts of rainfall in local areas and ended before evening. Lau et al. (2000) pointed out that the 1998 east Asian summer monsoon developed over the entire South China Sea region during 20–25 May. The onset of the summer monsoon near the Taiwan area began on 25 May, when the first Mei-yu front (not shown) migrated to the vicinity of Taiwan and brought light rainfall to the island during both daytime and nighttime hours over the next few days (see Fig. 3). The front weakened shortly after 28 May. The majority of the heavy rainfall events of the 1998 Mei-yu season did not occur until 1 June, when a Mei-yu front moved over southern Taiwan. Many MCSs developed along the Mei-yu front, over the ocean off the southeastern coast of China, and moved toward southern Taiwan, resulting in heavy precipitation. Precipitation fell mostly on the central mountainous areas and the southern part of Taiwan during this heavy-rainfall period that lasted until 11 June, which accounted for most of the rainfall of the 1998 Mei-yu season.

Figure 4 shows the diurnal variation of precipitation averaged during the 1998 Mei-yu season. Before the monsoon onset, rainfall occurred mainly during daytime hours (0800–2000 LST; Fig. 4a). A sharp peak of precipitation was observed between 1400 and 1800 LST,

---

[1] The $\sigma = 0.995, 0.985, 0.975, 0.965, 0.955, 0.945, 0.935, 0.915,$ 0.895, 0.87, 0.825, 0.775, 0.725, 0.675, 0.625, 0.575, 0.525, 0.475, 0.425, 0.375, 0.325, 0.275, 0.225, 0.175, 0.125, 0.075, and 0.025. The vertical coordinate σ is defined as $(p - p_t)/(p_s - p_t)$, where p is pressure, p_s is surface pressure, and p_t is a constant pressure at the top of the model (100 hPa).

[2] The stations use the tipping-bucket rain gauge for rainfall measurement, with a resolution of 0.5 mm.
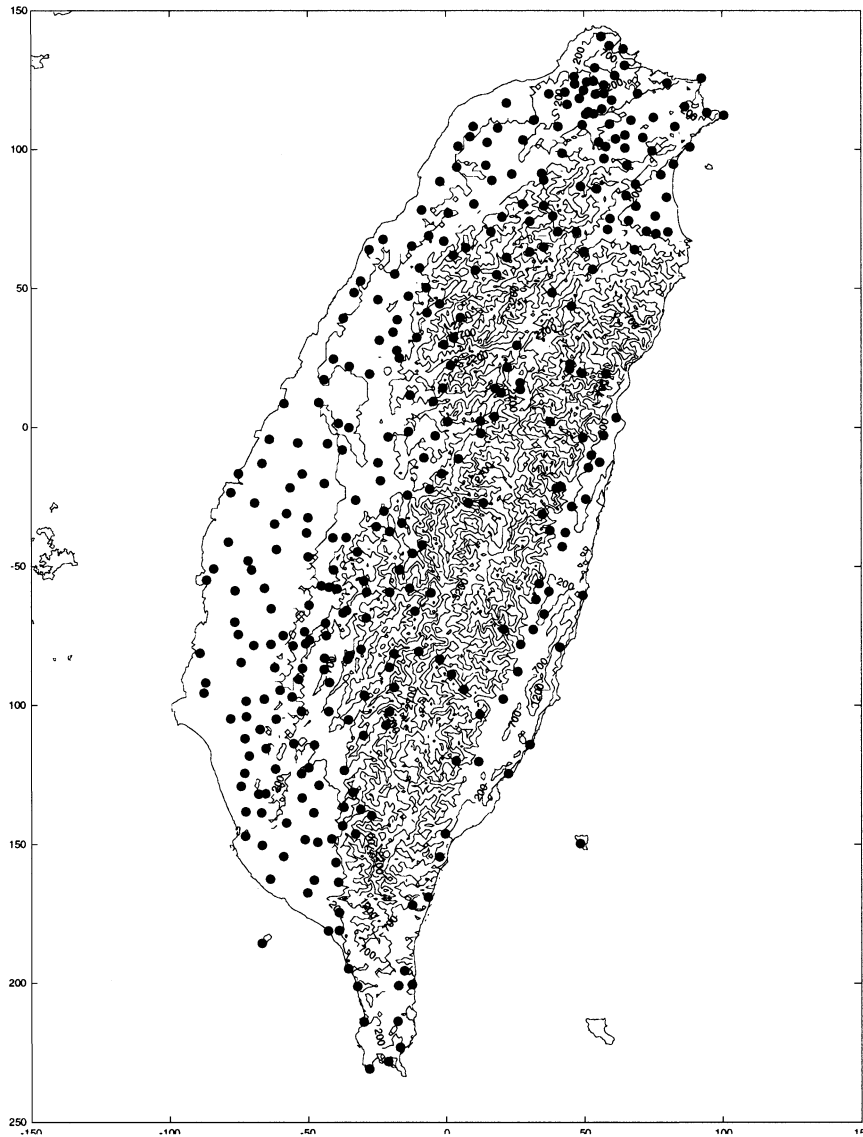
FIG. 2. The locations of the 342 rain gauge stations in Taiwan. Terrain height (thin lines) starts at 200 m, with a contour interval of 500 m.

with a maximum at 1600 LST. This is attributed to strong solar heating in the afternoon that resulted in the development of low-level unstable air and anabatic winds. Orographic lifting of the anabatic winds also played an important role in triggering and enhancing the convection (Yeh and Chen 1998), because the storms appeared to be initiated primarily over the slopes. This is suggested by Fig. 4a, which shows that rainfall tended to occur more frequently over the slopes (stations with medium altitudes) than over the lowlands. The thunderstorms vanished and the rainfall stopped in the evening, as a result of evaporative cooling and longwave radiational cooling after sunset. Yeh and Chen (1998) pointed out that the development of katabatic winds in the evening was also important in dissipating the storms.

It is also noted that another minor peak of the diurnal rainfall occurred around 0900–1000 LST. In contrast to the maximum rainfall in the afternoon, more precipitation was observed over the lowlands than over the mountainous regions around this time. This suggests that weak convection could sometimes form early in the morning. The resulting light rainfall, coupled with the development of sea breezes, meant that stations over the lowlands had a better chance of receiving more rainfall than the mountainous regions during early daytime hours.

The diurnal variations of hourly rainfall after the monsoon onset (Fig. 4b) were very different from those before the onset. The figure shows that rainfall occurred during both daytime and nighttime hours, with no sharp
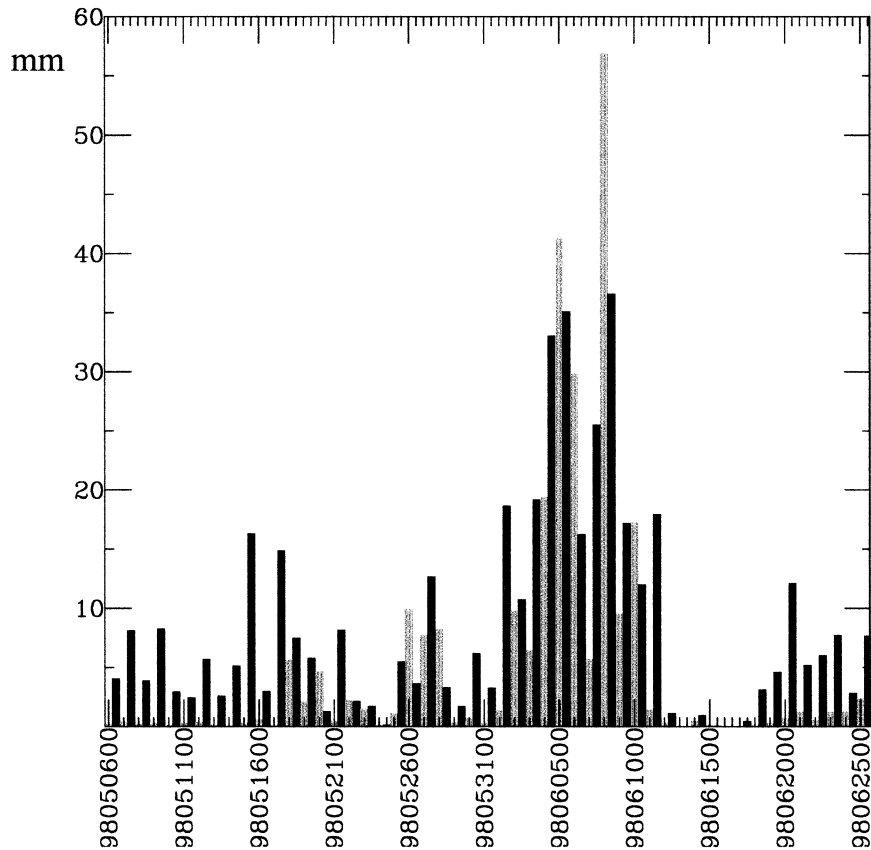
FIG. 3. Twelve-hour accumulated precipitation averaged for the 342 rain gauge stations in Taiwan. Ending times are from 0000 UTC 6 May to 1200 UTC 25 Jun 1998 at a 12-h interval. The bars in black denote rainfall accumulated from 0000 to 1200 UTC (daytime, 0800–2000 LST), and those in gray represent rainfall accumulated from 1200 to 0000 UTC (nighttime, 2000–0800 LST).

peak. A gentle maximum could be found during the afternoon hours, with more precipitation recorded over mountainous regions than over the lowlands. Between 0000 and 1000 LST, more rainfall was observed over the lowlands than over the mountainous regions. It is therefore clear that, after the monsoon onset, Mei-yu fronts (and/or the associated MCSs) produced rainfall during both daytime and nighttime hours. In addition, local circulations that resulted from the interaction of synoptic flow, the mountains, and strong solar heating could further enhance rainfall in the afternoon, especially over the slopes.

Figure 5 presents accumulated rainfall distribution over the island for daytime (0000–1200 UTC, 0800–2000 LST) and nighttime (1200–2400 UTC, 2000–0800 LST) hours for the ~2-month period. Before the monsoon onset, rainfall occurred predominantly during the day and mainly over mountain slopes, as discussed earlier. Accumulated premonsoon daytime rainfall in northern Taiwan reached a maximum of greater than 200 mm over this period. After the monsoon onset, precipitation became much heavier, especially over southern Taiwan (see Fig. 5; please note the difference

in shading contour intervals). This is because the flow to the southwest of Taiwan turned from weak southerly to stronger southwesterly after the onset, and such flow with moist air resulted in the development of many MCSs along the southern side of the Mei-yu fronts. Some of these MCSs moved over the southern part of Taiwan, producing heavy rainfall. Rainfall amounts during this time period were more evenly distributed between daytime and nighttime hours. In addition, daytime precipitation appears to take place mostly along the mountain slopes, whereas the nighttime precipitation is more evenly distributed in the east–west direction; however, the amount increases southward over southern Taiwan. This again suggests that the mountain range plays an important role in enhancing the daytime precipitation but has relatively small influence on the nighttime precipitation.

4. Precipitation verification in MM5

a. The verification method

In this study, we verify the precipitation forecasts of the nested domain (15 km) on the model grids. Because
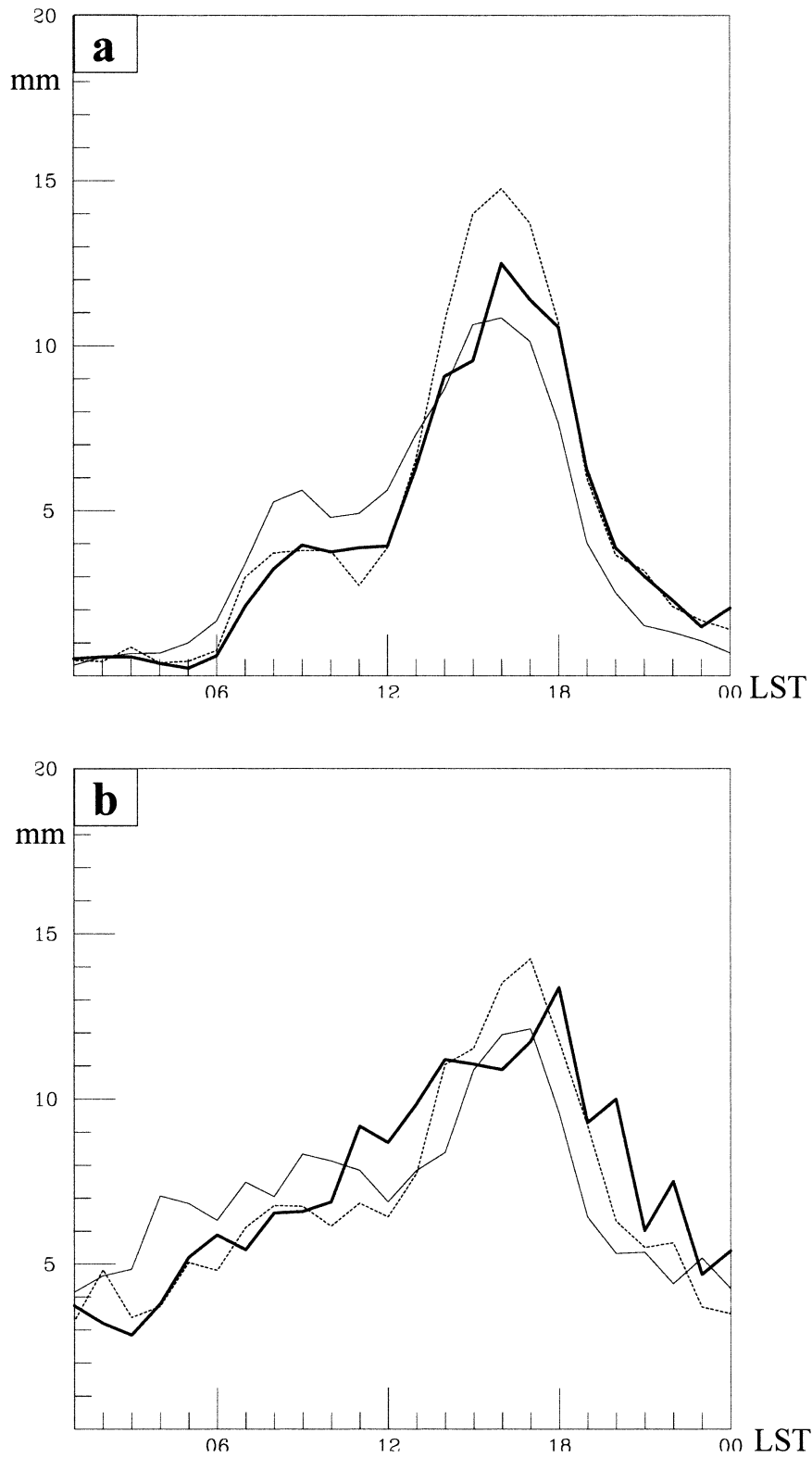
Fig. 4. Diurnal variations of hourly rainfall averaged over three groups of stations that are classified by station altitude; thin, dashed, and thick curves represent the groups of stations with low (0–200 m), medium (200–1200 m), and high (>1200 m) terrain height, respectively. The rainfall is averaged for (a) 5–25 May (before the monsoon onset) and (b) 26 May–25 Jun (after the monsoon onset) 1998.
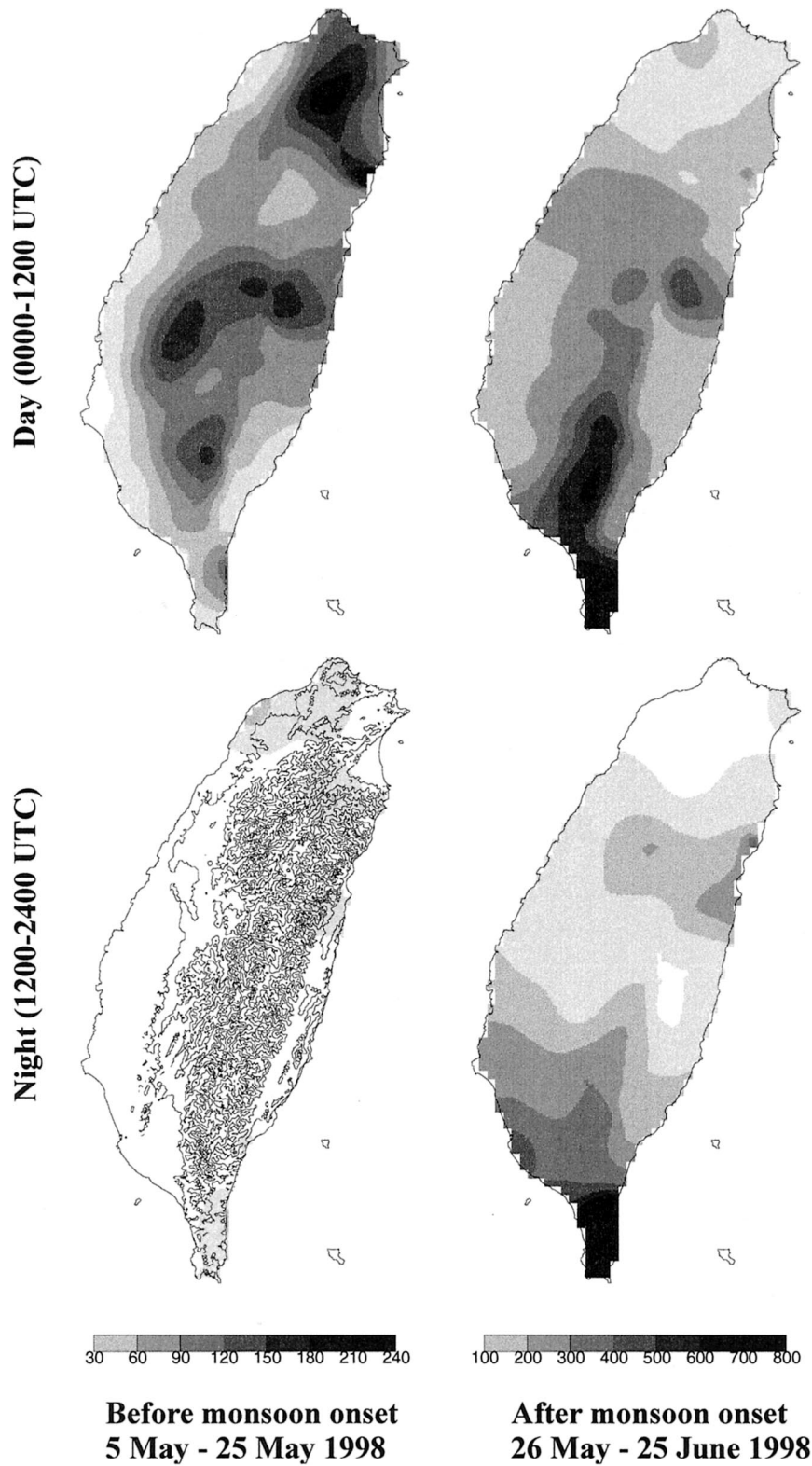
FIG. 5. Observed rainfall (mm) accumulated during daytime and nighttime periods for (left) 5–25 May and (right) 26 May–25 Jun 1998. Note that the shading scales are different for the two columns. Terrain height (contour lines starting at 200 m with a 500-m interval) is also shown in the lower-left panel.

the rain gauge stations are irregularly distributed around the grid points over the island, the observed rainfall data have to be processed before we proceed with the verification study. To provide rainfall observation at a resolution compatible with the model, the rain gauge data that are located within a 15-km square, centered at a grid point of the 15-km domain, are averaged to represent the observed rainfall amount at that grid point. These processed data are then compared with the model precipitation amount at the same grid point, over the same time period. The result registers as a sample for the verification. Because there are 141 grid points over the land area of Taiwan in the 15-km domain, each MM5 run would create, at most, 141 samples for a specified time interval. In some cases, fewer samples may be obtained because of missing observational data or low rain gauge density over a certain region of the domain (particularly over high mountains and over eastern Taiwan). In these situations, a symbol of AA is used to designate the "absence" of observational data.

Using samples collected from 100 runs of the 15-km domain in 50 days (5 May–25 June 1998), we calculated the equitable threat score (ETS; Schaefer 1990) of the precipitation forecast for the 1998 Mei-yu season. The definition of ETS is the same as the standard threat score except that the numerator (H) and the denominator ($F + O - H$) are both subtracted by the expected number of hits[3] in a random forecast R:

$$ETS = \frac{H - R}{F + O - H - R},\qquad (1)$$

where H is the number of hits, and F and O are the numbers of samples in which the precipitation amounts are greater than the specified threshold in forecast and observation, respectively; the random forecast $R = FO/N$, where N is the total number of points being verified. The thresholds used in this study include 0.3, 2.5, 5, 10, 15, 25, 35, and 50 mm of precipitation. The model bias is also calculated by $B = F/O$.

The precipitation verifications are presented in the following subsections. To study the characteristics of rainfall predictions for different model initial times, geographical locations, and climatic circumstances, the verification samples were stratified into different groups.

b. ETS for different initial times

As noted earlier, because the observed precipitation distribution shows different characteristics between daytime and nighttime, our interest was in evaluating the model performance for daytime and nighttime, separately. Moreover, we noted that the model performance appears to differ for runs initialized at 0000 UTC (here-

---

[3] When both the observed and forecast rainfall amounts are greater than the specified threshold, it represents a hit.
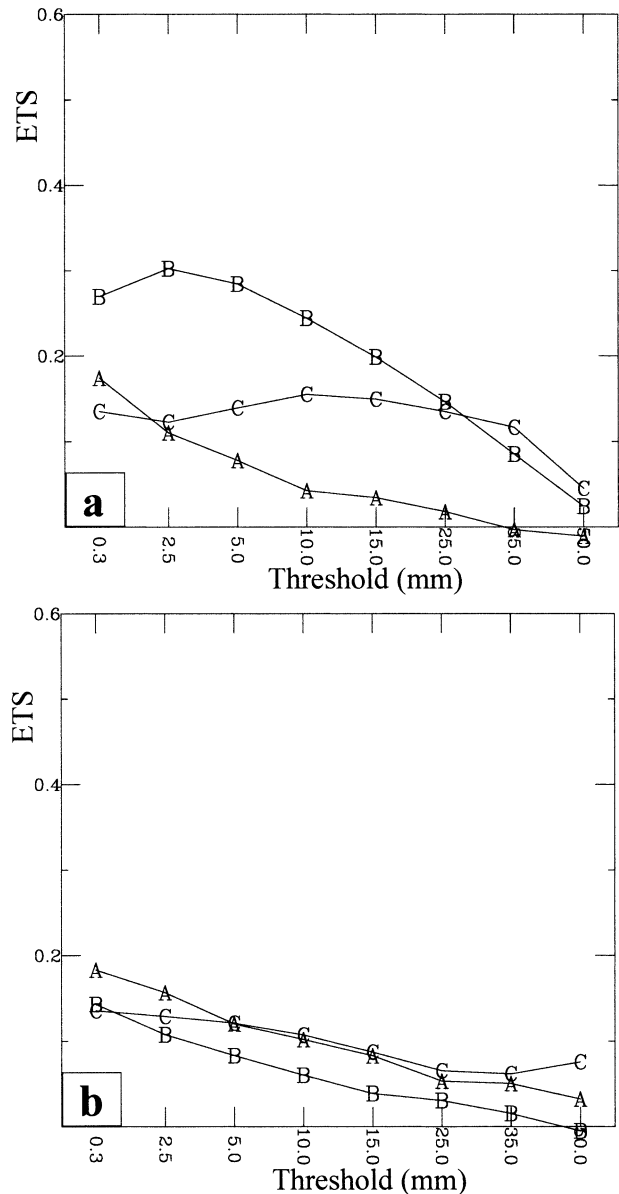

Fig. 6. The ETS of precipitation forecasts vs various thresholds (mm) for (a) the 0000 UTC runs and (b) the 1200 UTC runs, during the 1998 Mei-yu season. Three curves represent different verification periods of the model simulation. Curves A, B, and C denote scores for the 0–12-, 12–24-, and 24–36-h accumulated rainfall forecasts, respectively.

inafter referred to as 0000 UTC runs) versus 1200 UTC (hereinafter referred to as 1200 UTC runs). For these reasons, we divided the verification samples into two groups (0000 UTC and 1200 UTC initial times) and calculated the ETS for each group separately (Fig. 6). The overall performance of the model system on precipitation forecasts during the 1998 Mei-yu season can be estimated by simply averaging the ETS scores of the two groups.

Figure 6a shows the ETS computed from the real-

TABLE 1. The averaged amount of global soundings received by the CWB from 5 May to 20 Jun 1998.

	0000 UTC	0600 UTC	1200 UTC	1800 UTC
Soundings	624.6	77.1	564.6	73.0
Std dev	10.0	3.8	13.9	4.3

time MM5 forecasts for the 0000 UTC runs. The number of sample points that were verified in this calculation exceeds 6000. The three curves (A, B, and C) represent the ETS scores for the 12-h accumulated rainfall forecasts of time periods at 0–12, 12–24, and 24–36 h, respectively. It is found that the 12–24-h rainfall forecast (B curve) gave the highest scores for almost all thresholds, and the highest ETS exceeded 0.3 at the 2.5-mm threshold. The ETSs dropped as the threshold amounts increased. In other words, the MM5 model did a reasonably accurate job in forecasting the chances of precipitation but had lower forecast skill in predicting the amount of rainfall, especially when it was heavy. This kind of behavior is common to almost all research and operational models over diverse geographical areas (Mesinger 1996; Colle et al. 1999). As for the precipitation forecasts between 24 and 36 h (C curve), the scores were lower than 0.2 for all thresholds. It is clear that the model's skill in rainfall forecasts decreased after 24 h. This is consistent with the results of Colle et al. (1999) who found that MM5 performed best in precipitation forecasting at 18 h. It appears that the model QPF skill for medium precipitation thresholds was slightly higher than those at small and large thresholds for the 24–36-h forecasts. Last, it is obvious that the model's QPF skill was low during the first 12-h forecast. A possible explanation for such poor performance is that the model was still going through its initial adjustment, during the first 12-h forecast. It is well known that the model generally takes 6–12 h to develop realistic cloud and rainfall patterns from the smooth large-scale initial condition, which is known as the precipitation spinup problem.

The 1200 UTC runs (Fig. 6b) produced less accurate forecasts for both the 12–24-h and 24–36-h accumulated rainfall than did the 0000 UTC runs. The ETS scores of these runs were all lower than 0.15. There are at least three factors that may account for this difference. First, the averaged amount of upper-air sounding data collected at 0000 UTC was about 10% greater than that collected at 1200 UTC, during this ~2-month period (see sounding statistics in Table 1, for example). Although most of the above-noted differences in sounding data occurred over the Tropics and the Southern Hemisphere, there were still some differences over the continent of Asia (not shown). As a result, better initial conditions (both from the first guess of the global model, and from the objective analysis of the mesoscale model) of the 0000 UTC runs may produce better forecasts than the 1200 UTC runs. Second, in east Asia, the atmosphere at 1200 UTC is more likely to be in a

disturbed state at the mesoscale than it is at 0000 UTC, thus introducing initial value errors on scales that may be transparent to the synoptic data. Last, the CAA–CWB real-time MM5 system had better prediction skill for nighttime precipitation than for daytime precipitation. For example, the 12–24-h forecast, which represented the nighttime precipitation forecast (2000–0800 LST) for the 0000 UTC runs (Fig. 6a), performed better than the 24–36-h rainfall forecast (daytime, 0800–2000 LST). For the 1200 UTC runs, though generally inferior to that from the 0000 UTC runs, the 24–36-h forecast (2000–0800 LST) was slightly better than the 12–24-h forecast (0800–2000 LST). As stated earlier, the model's accuracy in rainfall forecasts was best between 12 and 24 h, during which the 1200 UTC runs had difficulty in predicting the daytime precipitation. Because daytime rainfall during this season was usually associated with diurnal thermal forcing and orographic lifting, this might indicate deficiencies in the parameterization of convective triggering in the cumulus parameterization scheme. Additional studies need to be performed to investigate whether improvement of grid resolution, improvement in convective triggering parameterization, and improvement of other physics processes (e.g., PBL parameterization) can help the model performance.

The bias scores of the precipitation forecast for the 0000 UTC runs (Fig. 7a) were close to 1 for both the 0–12-h and 12–24-h accumulated rainfall forecasts, except at the largest threshold (50 mm). For the 24–36-h accumulated rainfall forecasts, the model tended to underforecast the precipitation at smaller thresholds and overforecast at large thresholds (for 35 and 50 mm). All precipitation was underforecast during the three 12-h time periods for the 1200 UTC runs, except for the 12–24-h forecast at the highest threshold (Fig. 7b). It is noted that daytime precipitation (C curve of Fig. 7a and B curve of Fig. 7b) was generally underpredicted because fewer convection events were forecast by the model. Nighttime precipitation was captured better by the model in the 0000 UTC runs than in the 1200 UTC runs. It is interesting that the 0–12-h forecast from the 0000 UTC runs had a relatively low ETS score but a very good bias score. This result implies that the total number of grid points receiving precipitation above certain thresholds is compatible with the observed precipitation, but with large differences in the horizontal distribution of precipitation.

c. Spatial variation of ETS

To investigate the relationship between the rainfall forecast accuracy and the Taiwan terrain, the ETS was displayed at each grid point (with 15-km spacing) over Taiwan. Unlike the previous definition of ETS, which included samples in space and time, the ETS in this section only contained samples in time. Because the precipitation forecast generally had the highest ETS at
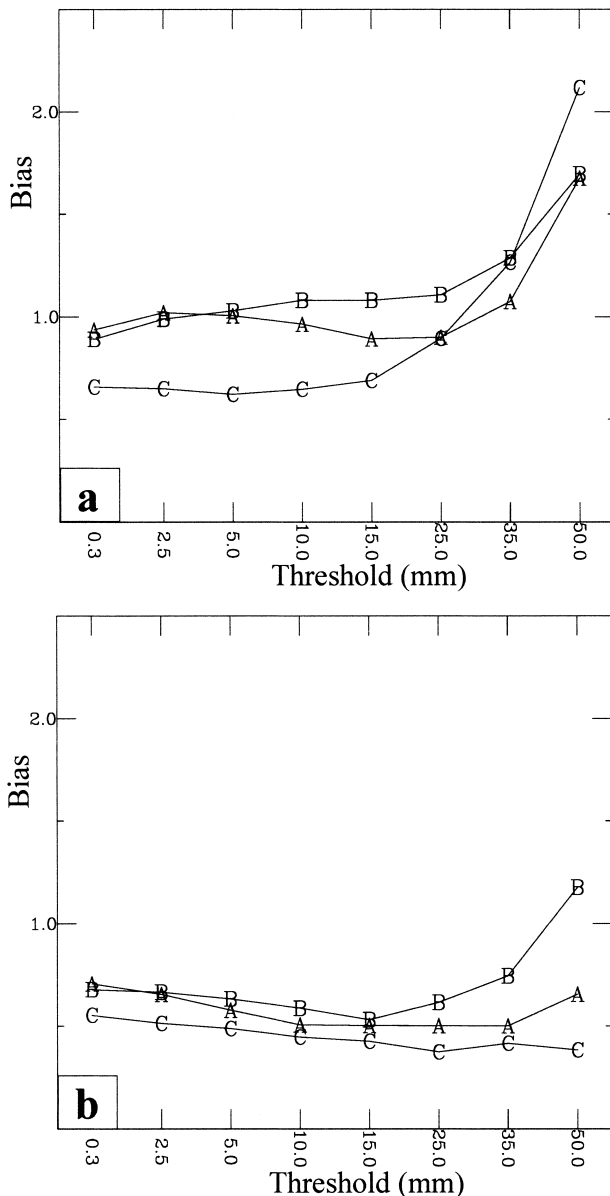
FIG. 7. Same as Fig. 6, but for the bias.

Taiwan. The scores were relatively low in the northwestern and the southeastern coastal zones. This result is consistent with the experiences of local forecasters who point out that model rainfall forecasts near these two regions usually have low accuracy. The cause of the inaccuracy is unclear, but the unique mountainous terrain is considered to be one factor. Over the high mountainous areas, the ETSs were also very low, around 0.2 in general. The poor performance could be related to lower model skill in forecasting over mountainous regions and to the low density of rain gauge observations over the high terrain.

For the 1200 UTC runs (Fig. 8b), the ETSs of the 12–24-h rainfall forecast (corresponding to 0800–2000 LST) were all very low over the island. The lowest scores (<0.1) were mainly found over the steep slopes of the CMR, which were also the regions in which most of the daytime precipitation took place (see Fig. 5). The corresponding figure of the bias score further indicates that precipitation was mostly underforecast over those areas (not shown). For higher terrain areas (>1200 m, in general), scores were slightly larger, except at those grid points (indicated by AA) where no observation was found within the 15-km box. These higher-score regions were, in fact, a result of overprediction by the model, which will be discussed in the next subsection.

The ETSs of the 24–36-h rainfall forecast computed for the 0000 UTC runs (corresponding to 0800–2000 LST) were mostly lower than 0.3, except over a few small regions (Fig. 8c). The regions with poor forecast skill (ETS < 0.1) were generally located over the eastern and western slopes of the CMR and over the northwestern coastal zone. There are two factors that could contribute to the differences in skill between the 12–24-h and 24–36-h rainfall forecasts of the 0000 UTC runs. First, the model performance of rainfall forecasts reached its peak by 24 h, and decreased after that. Second, because this forecast time period was during the local daytime, the MM5 had difficulty predicting rainfall produced by local, thermally forced convection, which occurred especially over the slopes.

Figure 8d presents the ETSs of the 24–36-h rainfall forecast for the 1200 UTC runs (corresponding to 2000–0800 LST). The scores were very low (<0.1) at nearly all the grid points west of the CMR. There were also a few regions that had low ETSs in the eastern coastal zone. The difficulty in obtaining accurate model predictions for these areas has been discussed. Over the northern and northeastern island, the model did a relatively good job in predicting the rainfall. The forecast time period of Fig. 8d was during the local nighttime, same as in Fig. 8a, but the scores were considerably lower than those of the 12–24-h forecasts of the 0000 UTC runs. This is because of the lower forecast skill of the 1200 UTC runs, as discussed earlier. Furthermore, because the forecasts of the previous 12 h (12–24 h) during daytime already had low accuracy (Fig. 8b), it is not surprising that the model skill scores were even
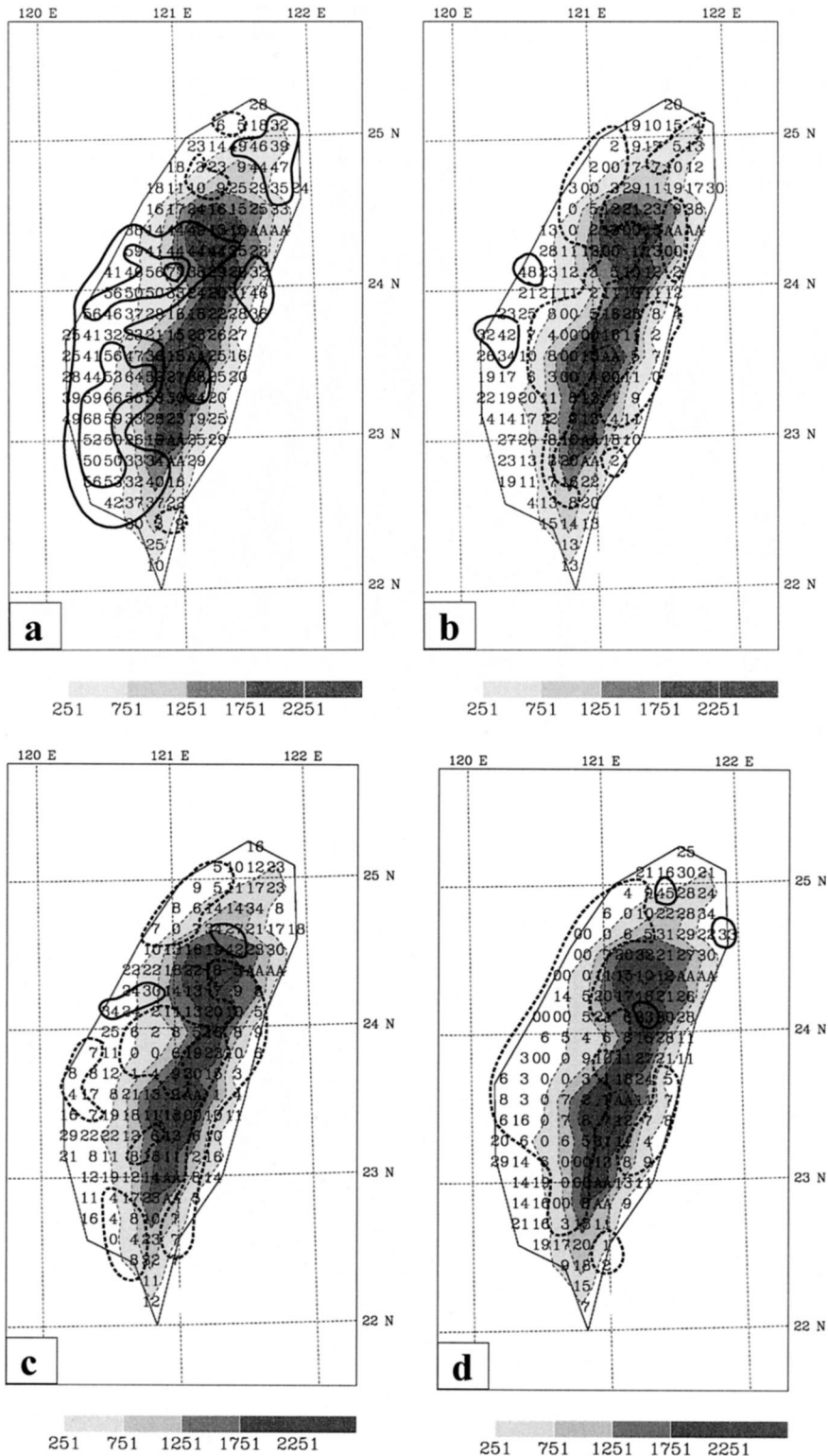
the 2.5-mm threshold as discussed earlier, we will use this threshold to illustrate the verification result. The ETS is also shown separately for the 0000 UTC runs and for the 1200 UTC runs in order to diagnose different characteristics between daytime and nighttime rainfall prediction. Figure 8a shows that the ETS of the 12–24-h rainfall forecast for the 0000 UTC runs (corresponding to 2000–0800 LST) produced good results over most of the grid points over the island. Many grid points over the lowlands of central and southern Taiwan had scores greater than 0.3, with some locations even exceeding 0.5. Over the northern and eastern portions of the island, the ETSs were, in general, lower than 0.3, except for a few regions such as northeastern

FIG. 8. The ETS ($\times$ 100) of precipitation forecasts averaged at grid points over Taiwan for the 2.5-mm threshold: 12–24-h rainfall forecasts for (a) the 0000 UTC runs and (b) the 1200 UTC runs, and 24–36-h rainfall forecasts for (c) the 0000 UTC runs and (d) the 1200 UTC runs. Bold lines denote ETS at 0.1, 0.3, 0.5, and 0.7 (0.1 lines are dashed). Thin dashed lines with shading represent model terrain heights from 250 to 2250 m at a 500-m interval. Code AA represents missing data.

lower for the subsequent 12-h forecasts (24–36-h rainfall). A comparison between Figs. 8b and 8d shows that scores over the southwestern lowlands decreased from the 12–24-h forecast to the 24–36-h forecast while the scores over the mountainous regions, including the northeast, increased slightly. In general, the model's accuracy in the precipitation forecast decreased after 24 h. However, because the difference of model performance between daytime and nighttime is more pronounced than the impact of forecast length (12–24- vs 24–36-h forecast), the scores on the slopes during nighttime hours (24–36 h) were higher than daytime hours (12–24 h). Even so, the overall skill of the 24–36-h (nighttime) rainfall forecast was still slightly higher than that of the 12–24-h (daytime) forecast at the 2.5-mm threshold and was notably better at larger thresholds (C and B curves in Fig. 6b). The fact that the 24–36-h forecast outperformed the 12–24-h forecast for the 1200 UTC runs, together with the results of dramatically decreased skills from 12–24-h forecast to 24–36-h forecast of the 0000 UTC runs, clearly indicates that the model had much lower skill in predicting daytime precipitation than nighttime precipitation.

d. ETS with respect to terrain height

To examine further the model performance with respect to terrain height, ETSs are averaged for three groups of grid points that are classified according to their terrain elevation. Only the results of the 12–24-h precipitation forecasts from the 0000 UTC runs are shown here; the others gave similar results. Group L (low) is for the grid points with terrain heights lower than 200 m, M (medium) is for those between 200 and 1200 m, and H (high) is for those higher than 1200 m. Group M represents mountain slopes, and group H denotes highland regions. As shown in Fig. 9a, for the 0000 UTC runs, ETSs for low terrain (L curve) were highest for nearly all thresholds among the three groups. The highest score was very close to 0.4 at the 2.5-mm threshold. The skill score decreased rapidly at rainfall thresholds greater than 15 mm. For medium (M curve) and high (H curve) terrain regions, the scores were very close, except for the large thresholds (i.e., >25 mm), for which the H curve was higher than the M curve. This result is related to the fact that the model generally overpredicted precipitation over the high terrain areas, and it increased ETSs slightly by increasing the number of hits [H in Eq. (1)]. As we see from Fig. 9b, their bias scores were much larger than unity, which suggests that the forecasts were of low reference value.

Bias scores for the 12–24-h rainfall forecasts of the 0000 UTC runs were slightly lower than 1 for low and medium terrain-height regions and were considerably larger than unity for high terrain areas, especially at large thresholds (Fig. 9b). This result suggests that the model tended to underpredict slightly the rainfall occurrence for all the thresholds at grid points lower than
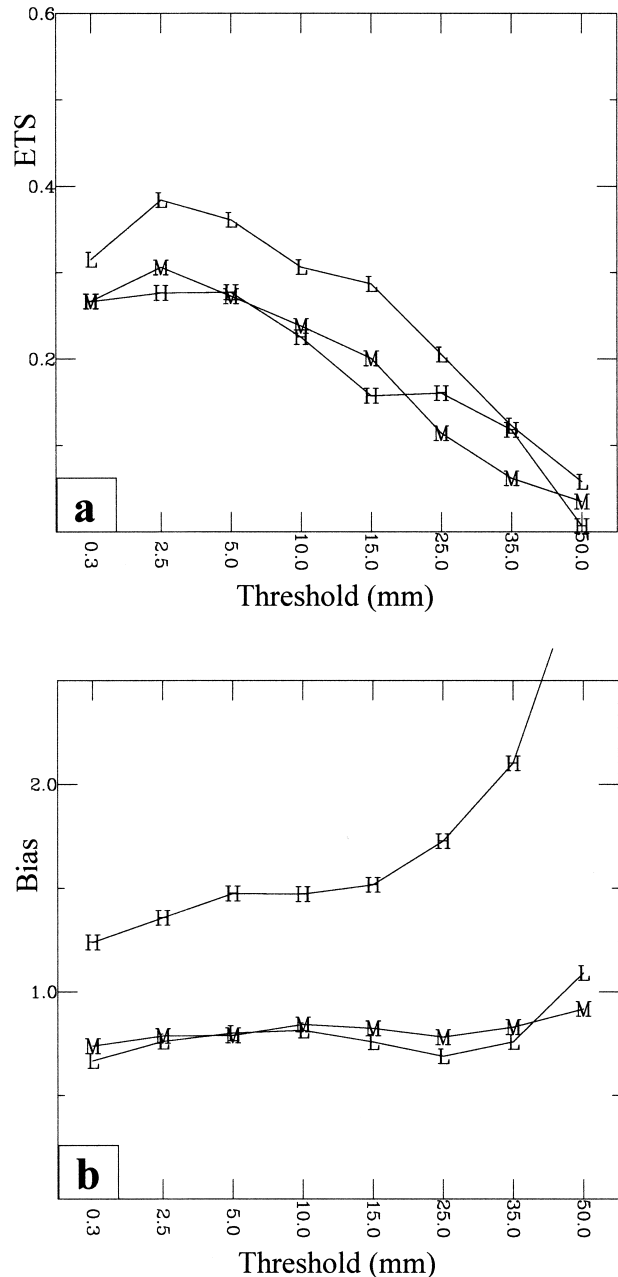

FIG. 9. The (a) ETS and (b) bias averaged for three groups of grid points that are classified by their terrain heights. Curves L, M, and H denote scores for the groups with low (0–200 m), medium (200–1200 m), and high (>1200 m) terrain height, respectively, shown vs various rainfall thresholds for the 12–24-h precipitation forecasts from the 0000 UTC runs.

1200 m. For highland regions, MM5 overpredicted precipitation events.

The ETS results given above indicate that the model performed better over the lowlands than over the mountainous areas (slopes and highlands). The bias score further shows that the model generally overpredicted rainfall over the high terrain area (>1200 m). This might

have resulted from excessive upward forcing generated by the 15-km MM5 at high altitude, due to most rainfall in that area being in a resolvable scale (not shown). In addition to the aforementioned deficiency in the model physics processes, the problem is also related to the fact that the 15-km model is not of high enough resolution to represent the real terrain (and their gradients) that may be responsible for the trigger of convection (cf. Fig. 1b and Fig. 2). Note that the overprediction of rainfall over the high terrain regions might also be attributed to the fact that there were fewer observations available to verify model simulations at those locations. However, because those grid points without sufficient observational data were excluded from the samples, the lack of data should not be a major factor. Further investigation should be carried out to study the forecast problem at the high mountain regions (>1200 m) and to identify ways to improve the forecasts.

e. ETS before and after the monsoon onset

Another interesting investigation we conducted was to study the performance of MM5 in rainfall prediction before and after the onset of the summer monsoon (25 May 1998). We divided the samples into two groups, one before the onset (group B) and the other after the onset (group A). Figure 10a shows the scores for the 12–24-h rainfall forecast from the 0000 UTC runs. We found that the scores were considerably higher for curve A than for curve B at all thresholds. The bias scores indicate that the model overpredicted nighttime rainfall before the onset, especially for the larger thresholds, but it performed much better for the nighttime precipitation after the onset[4] (Fig. 10b). For the 1200 UTC runs, the scores were lower, but the difference of ETSs between groups A and B was similar to that of the 0000 UTC runs (not shown). As we pointed out earlier, daytime precipitation before the onset was mostly associated with afternoon thunderstorms, which resulted in poor performance of the 12–24-h rainfall forecast for the 1200 UTC runs. Daytime rainfall forecasts improved slightly after the monsoon onset, because more rainfall events were associated with large-scale forcing at that time. This result further suggests that MM5 has better skill in predicting rainfall that resulted from the Mei-yu fronts (or MCSs developed along the Mei-yu fronts) than in predicting precipitation associated with the locally forced convection.

5. Discussion and summary

This study presented precipitation verification in the Taiwan area for a prototype real-time mesoscale prediction system during the 1998 Mei-yu season. To our knowledge, this is the first time the accuracy of a real-

---

[4] It is important to note that before the onset there was very little nighttime precipitation (see Figs. 3 and 5).
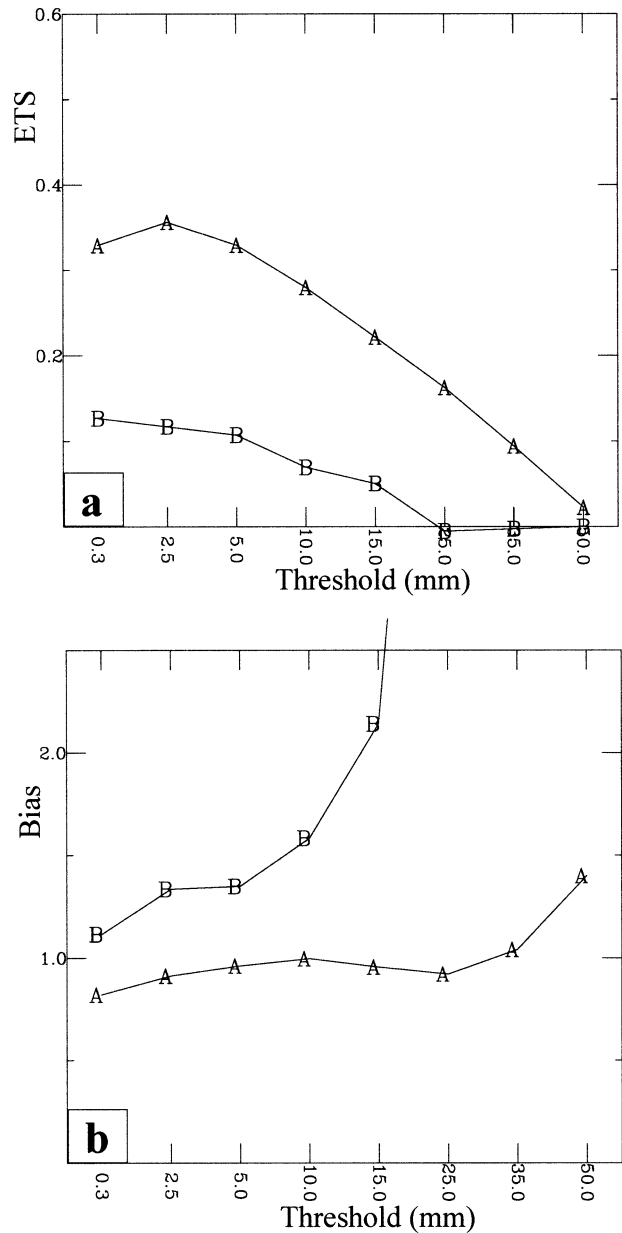

FIG. 10. The (a) ETS and (b) bias averaged for two groups of samples: one for the runs before the monsoon onset (curve B) and the other after the onset (curve A), shown vs various rainfall thresholds for the 12–24-h precipitation forecasts from the 0000 UTC runs.

time mesoscale model in quantitative precipitation forecasting has been evaluated in Taiwan. Observations show that the onset of the east Asian summer monsoon of 1998 near the Taiwan area occurred on 25 May, when the first Mei-yu front reached Taiwan and brought light rain to the island during both daytime and nighttime. Before the onset, precipitation over the Taiwan area occurred only during the daytime hours and was mostly associated with afternoon thunderstorms. One of the main causes of the thunderstorms was strong solar heating in the afternoon. In addition, orographic lifting also

played an important role in triggering and enhancing the convection, because most of the storms were initiated over the mountain slopes. The major rainfall events of the 1998 Mei-yu season were mostly confined to the time period of 1–11 June, during which many mesoscale convective systems developed along the Mei-yu fronts and moved toward southern Taiwan, producing a large amount of precipitation over the southern area. The distribution of rainfall pattern between day and night indicates that daytime precipitation tended to be modulated by the mountains and occurred along the slopes of the Central Mountain Range. The nighttime precipitation had a more uniform distribution over the island (with minimal mountain modulation) with a tendency for increasing rainfall southward.

The verification of model precipitation forecasts shows that the overall performance of the 15-km MM5 as measured by equitable threat score during the 1998 Mei-yu season was relatively low in the Taiwan area. Averaged over the entire verification period for all forecasts, the highest score was about 0.2 at the 2.5-mm threshold. One important reason for the low ETS is because our precipitation verification was done for a warm season, which is known to be the most difficult period for QPF. The ETS was still relatively low when compared with scores for the NCEP Eta and Nested Grid Models, which were greater than 0.3 at the same threshold over the U.S. continent for 0.5 yr (March–August, Mesinger 1996). Several reasons may exist for this result. First, the complex and steep terrain of Taiwan made it difficult for a 15-km model to predict realistic rainfall associated with small-scale convection that was driven by local forcings, such as thermal effect and orographic lifting. In addition, the lack of observational data over the surrounding ocean placed a strong limitation on the quality of the model's initial data. Last, it is important to note that our verification was done for 12-h rainfall forecasts, while NCEP's ETS was computed for 24-h rainfall forecasts.

When stratified according to different model initialization times, the ETS shows that scores for the runs initialized at 0000 UTC (the 0000 UTC runs) were considerably higher than those initialized at 1200 UTC (the 1200 UTC runs). The reasons for this may be threefold. First, the initial conditions for the 0000 UTC runs were generally of better quality than those for the 1200 UTC runs, because more upper-air soundings were collected at 0000 UTC than at 1200 UTC (about 10% more). This resulted in a better model initial condition, and thus better performance, for the 0000 UTC runs. Second, in east Asia, the atmosphere at 1200 UTC (evening) is more likely to be in a disturbed state at the mesoscale than it is at 0000 UTC (morning), thus introducing initial-value errors on scales that may not be properly resolved by the synoptic data. Last, the prototype real-time mesoscale prediction system simulated better nighttime precipitation than daytime precipitation because daytime rainfall during this Mei-yu

season was often associated with local rain showers that were of relatively small scale. These convective systems were neither properly triggered by the model's subgrid-scale scheme nor properly simulated by the resolvable precipitation scheme. The best ETS of the MM5 model system (>0.3) was found for the 12–24-h (nighttime) rainfall forecast, at the 2.5-mm threshold for the 0000 UTC runs, and the skill scores dropped as the thresholds increased. The scores became lower for the 24–36-h forecast. Similar to the results of Colle et al. (1999), the model's accuracy in rainfall prediction peaked during the first 12–24 h, and decreased with time afterward.

Spatial distribution of ETSs of the 0000 UTC runs shows that the forecast accuracy of the model at 12–24 h (nighttime precipitation) was very good over the entire island, especially over the southwestern lowlands. To the contrary, the 24–36-h (daytime precipitation) forecast of the same runs performed poorly, particularly over the slopes of the CMR. This difference between the 12–24-h and 24–36-h rainfall forecasts is attributed to the fact that the model performance of rainfall forecasts reached its peak before 24 h, and the MM5 had low skill in predicting diurnally forced local convection during the daytime hours. For the 1200 UTC runs, the scores of the 12–24-h and 24–36-h forecasts were both very low. Detailed analyses revealed that scores over the southwestern lowlands decreased from the 12–24-h forecast to the 24–36-h forecast, which is attributed to the decrease in the model's forecast accuracy after 24 h. It was found, however, that the scores over the mountainous regions were slightly higher at 24–36 h than at 12–24 h. Because the former reflects nighttime hours and the latter reflects daytime hours, this indicates that the difference in model accuracy between daytime and nighttime is more pronounced than that between the two integration periods.

For daytime rainfall prediction, MM5's ETS was very low over the slopes of the CMR. This was because the model underforecast local convection that was forced by the combined effects of orographic lifting and solar heating. This is somewhat different from the results of Colle et al. (1999), who found that MM5 overpredicted rainfall on the windward slopes of the mountains. It is important to note that the verification by Colle et al. (1999) was performed during a cool season when synoptic forcing was dominant, whereas in our study local forcings were considered to be an important factor. Another issue is that Colle et al. (1999) did not examine the performance of rainfall prediction in terms of terrain height. As we found in this study, the model still underpredicted rainfall at heights lower than 1200 m. The overprediction occurred only at grid points higher than 1200 m. The analysis of ETSs with regard to terrain height also indicates that the model performed better over the lowlands than over mountainous areas (slopes and highlands). Last, it is documented that the ETSs were much higher after the monsoon onset than before

the onset. This is because the Mei-yu front and the associated MCSs produced most of the precipitation in the Taiwan area after the onset, whereas thermal forcing and orographic lifting were primarily responsible for rainfall before the onset.

This study clearly shows that there is a significant deficiency in the performance of precipitation parameterization for this version of the 15-km MM5 over Taiwan during the Mei-yu season. The model did not properly simulate convective rainfall associated with local forcings, such as solar heating and orographic lifting. It also produced excessive rainfall over the high mountain areas. By increasing the resolution to 5 km in the near future, we hope that the model will have a better chance to simulate those precipitation systems under a similar synoptic and mesoscale environment. In addition, future studies should focus on the improvement of the cumulus schemes and boundary layer parameterization. In particular, MM5's performance in modeling convective triggering due to local forcing needs to be improved. A possible solution is to improve the convective triggering parameterization based on the studies of Wee and Lee (2000).

REFERENCES

Akiyama, T., 1973: The large-scale aspects of the characteristic features of Baiu front. *Pap. Meteor. Geophys.,* **24,** 157–188.

Blackadar, A. K., 1979: High resolution models of the planetary boundary layer. *Advances in Environmental Science and Engineering.* Vol. 1, No. 1, J. Pfafflin and E. Ziegler, Eds., Gordon and Breach, 50–85.

Chen, G. T.-J., and C.-Y. Liang, 1992: A midlevel vortex observed in the Taiwan Area Mesoscale Experiment (TAMEX). *J. Meteor. Soc. Japan,* **70,** 25–41.

Chen, S.-J., Y.-H. Kuo, W. Wang, Z.-Y. Tao, and B. Cui, 1998: A modeling case study of heavy rainstorms along the Mei-yu front. *Mon. Wea. Rev.,* **126,** 2331–2351.

Chen, Y.-L., 1993: Some synoptic-scale aspects of the surface fronts over southern China during TAMEX. *Mon. Wea. Rev.,* **121,** 50–64.

——, and N. B.-F. Hui, 1990: Analysis of a shallow front during the Taiwan Area Mesoscale Experiment. *Mon. Wea. Rev.,* **118,** 2649–2667.

Colle, B. A., K. J. Westrick, and C. F. Mass, 1999: Evaluation of MM5 and Eta-10 precipitation forecasts over the Pacific Northwest during the cool season. *Wea. Forecasting,* **14,** 137–154.

Ding, Y.-H., 1992: Summer monsoon rainfalls in China. *J. Meteor. Soc. Japan,* **70,** 337–396.

Dudhia, J., 1993: A nonhydrostatic version of the Penn State–NCAR Mesoscale Model: Validation tests and simulation of an Atlantic cyclone and cold front. *Mon. Wea. Rev.,* **121,** 1493–1513.

Fritsch, J. M., and Coauthors, 1998: Quantitative precipitation forecasting: Report of the eighth prospectus development team, U.S. Weather Research Program. *Bull. Amer. Meteor. Soc.,* **79,** 285–299.

Grell, G. A., J. Dudhia, and D. R. Stauffer, 1994: A description of the Fifth Generation Penn State/NCAR Mesoscale Model (MM5). NCAR Tech. Note NCAR/TN-398+STR, 138 pp.

Jeng, B.-F., H.-J. Chen, S.-C. Lin, T.-M. Leou, M. S. Peng, S. W. Chang, W.-R. Hsu, and C.-P. Chang, 1991: The limited-area forecast systems at the Central Weather Bureau in Taiwan. *Wea. Forecasting,* **6,** 155–178.

Johnson, E. L., and B. G. Olsen, 1998: Assessment of quantitative precipitation forecasts. *Wea. Forecasting,* **13,** 75–83.

Kain, J. S., and J. M. Fritsch, 1993: Convective parameterization for mesoscale models: The Kain–Fritsch scheme. *The Representation of Cumulus Convection in Numerical Models, Meteor. Monogr.,* No. 46, Amer. Meteor. Soc., 165–177.

Kalnay, E., M. Kanamitsu, and W. E. Baker, 1990: Global numerical weather prediction at the National Meteorological Center. *Bull. Amer. Meteor. Soc.,* **71,** 1410–1428.

Kato, K., 1985: On the abrupt change in the structure of the Baiu front over the China continent in late May of 1979. *J. Meteor. Soc. Japan,* **63,** 20–35.

Kato, T., K. Kurihara, H. Seko, and K. Saito, 1998: Verification of the MRI-nonhydrostatic-model predicted rainfall during the 1996 Baiu season. *J. Meteor. Soc. Japan,* **76,** 719–735.

Klemp, J. B., and D. R. Durran, 1983: An upper boundary condition permitting internal gravity wave radiation in numerical mesoscale models. *Mon. Wea. Rev.,* **111,** 430–444.

Kuo, Y.-H., and F. T.-J. Chen, 1990: The Taiwan Area Mesoscale Experiment (TAMEX): An overview. *Bull. Amer. Meteor. Soc.,* **71,** 488–503.

Landis, R. C., 1994: Comments on "Forecasting in meteorology." *Bull. Amer. Meteor. Soc.,* **75,** 823–827.

Lau, K. M., and Coauthors, 2000: A report of the field operations and early results of the South China Sea Monsoon Experiment (SCSMEX). *Bull. Amer. Meteor. Soc.,* **81,** 1261–1270.

Li, J., Y.-L. Chen, and W.-C. Lee, 1997: Analysis of a heavy rainfall event during TAMEX. *Mon. Wea. Rev.,* **125,** 1060–1081.

Lin, Y.-J., R. W. Pasken, and H.-W. Chang, 1992: The structure of a subtropical prefrontal convective rainband. Part I: Mesoscale kinematic structure determined from dual-Doppler measurements. *Mon. Wea. Rev.,* **120,** 1816–1836.

Liou, C. S., and Coauthors, 1997: The second-generation global forecast system at the Central Weather Bureau in Taiwan. *Wea. Forecasting,* **12,** 653–663.

Mesinger, F., 1996: Improvements in quantitative precipitation forecasts with the Eta Regional Model at the National Centers for Environment Prediction: The 48-km upgrade. *Bull. Amer. Meteor. Soc.,* **77,** 2637–2649.

Olson, D. A., N. W. Junker, and B. Korty, 1995: Evaluation of 33 years of quantitative precipitation forecasting at the NMC. *Wea. Forecasting,* **10,** 498–511.

Ray, P. S., A. Robinson, and Y. Lin, 1991: Radar analysis of a TAMEX frontal system. *Mon. Wea. Rev.,* **119,** 2519–2539.

Schaefer, J. T., 1990: The critical success index as indicator of warning skill. *Wea. Forecasting,* **5,** 570–575.

Shuman, F. G., 1989: History of numerical weather prediction at the National Meteorological Center. *Wea. Forecasting,* **4,** 286–296.

Wang, C. T.-C., Y.-J. Lin, R. W. Pasken, and H. Shen, 1990: Characteristics of a subtropical squall line determined from TAMAX dual-Doppler data. Part I: Kinematic structure. *J. Atmos. Sci.,* **47,** 2357–2381.

Wee, T.-K., and D.-K. Lee, 2000: A comparative study of convective trigger functions in a cumulus parameterization. Preprints, *Int. Conf. on Mesoscale Convective Systems and Heavy Rain in East Asia,* Seoul, Korea, Korean Meteor. Soc., 255–260.

[Available from Korean Meteorological Society, c/o Dept. of Atmospheric Sciences, Seoul National University, Seoul 151–742 Korea.]

Wu, C.-C., and Y.-H. Kuo, 1999: Typhoons affecting Taiwan: Current understanding and future challenges. *Bull. Amer. Meteor. Soc.,* **80,** 67–80.

Yang, M.-J., F.-C. Chien, and M.-D. Cheng, 2000: Precipitation parameterization in a simulated Mei-yu front. *Terr. Atmos. Oceanic Sci.,* **11,** 393–422.

Yeh, H.-C., and Y.-L. Chen, 1998: Characteristics of rainfall distributions over Taiwan during the Taiwan Area Mesoscale Experiment (TAMEX). *J. Appl. Meteor.,* **37,** 1457–1469.